The EMBO Journal (2009) 28, 1878–1889 | © 2009 European Molecular Biology Organization | Some Rights Reserved 0261-4189/09
www.embojournal.org

THE EMBO JOURNAL

EMBO open

Screen for DNA-damage-responsive histone modifications identifies H3K9Ac and H3K56Ac in human cells

Jorrit V Tjeertes[1], Kyle M Miller[1,*] and Stephen P Jackson*

The Gurdon Institute, University of Cambridge, Cambridge, UK

Recognition and repair of damaged DNA occurs within the context of chromatin. The key protein components of chromatin are histones, whose post-translational modifications control diverse chromatin functions. Here, we report our findings from a large-scale screen for DNA-damage-responsive histone modifications in human cells. We have identified specific phosphorylations and acetylations on histone H3 that decrease in response to DNA damage. Significantly, we find that DNA-damage-induced changes in H3S10p, H3S28p and H3.3S31p are a consequence of cell-cycle re-positioning rather than DNA damage *per se*. In contrast, H3K9Ac and H3K56Ac, a mark previously uncharacterized in human cells, are rapidly and reversibly reduced in response to DNA damage. Finally, we show that the histone acetyl-transferase GCN5/KAT2A acetylates H3K56 *in vitro* and *in vivo*. Collectively, our data indicate that though most histone modifications do not change appreciably after genotoxic stress, H3K9Ac and H3K56Ac are reduced in response to DNA damage in human cells.

The EMBO Journal (2009) **28,** 1878–1889. doi:10.1038/emboj.2009.119; Published online 30 April 2009
Subject Categories: chromatin & transcription; genome stability & dynamics
Keywords: chromatin; DNA damage; H3K56Ac; histone PTMs

Introduction

Protection of an organism's genetic information is crucial for maintaining cell viability and averting pathologies, such as cancer (Aguilera and Gomez-Gonzalez, 2008). Cells possess surveillance systems, collectively termed as the DNA-damage response (DDR), to monitor and maintain genome stability. The DDR uses sensor proteins that recognize DNA damage, promote DNA repair and initiate 'checkpoint' events that control cell-cycle progression (Harper and Elledge, 2007). In human cells, DDR proteins include the PI3-kinase-related protein kinases (PIKKs) ataxia telangiectasia mutated (ATM), ATR (ATM and Rad3 related) and DNA-PK (DNA-dependent protein kinase). Upon activation, these kinases then trigger the phosphorylation of over 700 identified protein targets that regulate multiple cellular processes, including DNA repair, cell-cycle progression and transcription (Matsuoka *et al*, 2007). Well-characterized PIKK phosphorylation sites include Ser-15 of p53, Ser-966 of SMC1 and Ser-139 of H2AX.

Although analyses of the DDR have traditionally focused on the nature of the DNA damage itself, it is clear that the true initiating substrate for the DDR *in vivo* is damaged DNA in the context of chromatin (Downs *et al*, 2007; Groth *et al*, 2007; Escargueil *et al*, 2008). The basic unit of chromatin is the nucleosome, which contains approximately 146 base pairs of DNA wrapped around an octamer of eight core histones, comprising two copies each of the four core histones: H2A, H2B, H3 and H4. Chromatin functions are influenced by reversible histone post-translational modifications (PTMs), which include methylation, ubiquitylation, sumoylation, phosphorylation and acetylation (Kouzarides, 2007). Each of these reversible modifications is regulated by specific enzymes and has the capability of changing dynamically. For example, acetylation of lysines is accomplished by histone acetyl transferases (HATs), whereas deacetylation of lysines is catalysed by histone deacetylases (HDACs).

Histone modifications are best understood for their ability to regulate transcription (Berger, 2007), but it is becoming increasingly clear that histone PTMs also function in the DDR (Downs *et al*, 2007; Groth *et al*, 2007; Escargueil *et al*, 2008). The best characterized example of this is the PIKK-mediated phosphorylation of the C-terminal tail of histone H2AX (called γH2AX) (Rogakou *et al*, 1998), which is required to localize DDR proteins, such as MDC1 and 53BP1, to sites of DNA damage (Celeste *et al*, 2003; Bekker-Jensen *et al*, 2006; Stucki and Jackson, 2006). γH2AX also leads to the recruitment of chromatin-modifying enzymes, including HATs, HDACs, kinases, phosphatases, E3 ubiquitin ligases and chromatin remodeling complexes, to sites of DNA damage (Thiriet and Hayes, 2005; Huen *et al*, 2007; Kolas *et al*, 2007; Mailand *et al*, 2007). In addition, histone H2B Ser-14 is rapidly phosphorylated at the sites of DNA damage (Fernandez-Capetillo *et al*, 2004) and the maintenance of histone H3 phosphorylation on Thr-11 by CHK1 is lost upon DNA damage, which is implicated in the transcriptional regulation of certain genes that control cell-cycle progression (Shimada *et al*, 2008). Interestingly, after ultraviolet (UV) damage, all histones display a rapid hyper-acetlyation phase followed by a hypoacetylated state, although the specific histone marks that changed were unidentified (Ramanathan

*Corresponding authors. KM Miller or SP Jackson, The Gurdon Institute, University of Cambridge, Tennis Court Road, Cambridge CB2 1QN, UK. Tel.: +44 1223 334108; Fax: +44 1223 334089;
E-mails: k.miller@gurdon.cam.ac.uk or s.jackson@gurdon.cam.ac.uk
[1]These authors contributed equally to this work

Received: 16 January 2009; accepted: 26 March 2009; published online: 30 April 2009

and Smerdon, 1986). Additionally, H4K16 acetylation and H2A ubiquitylation have been shown to increase after ionizing radiation (IR) (Gupta *et al*, 2005; Huen *et al*, 2007; Mailand *et al*, 2007). Collectively, these data establish that multiple types of histone PTMs are involved in the DDR and, moreover, raise the prospect that additional DDR-responsive chromatin modifications await identification.

Results

Identification of DNA-damage-responsive histone PTMs

To screen for changes in histone modifications in response to DNA damage, we surveyed the global histone modification landscape with PTM-specific antibodies in extracts from human osteosarcoma (U2OS) cells untreated or treated with hydroxyurea (HU) or phleomycin. Fluorescence-activated cell sorting (FACS) analyses revealed that HU-treatment generated an enrichment of cells in S-phase, as expected because HU reduces deoxyribonucleotide levels, leading to S-phase arrest with DNA damage (Supplementary Figure 1A). In contrast, phleomycin treatment yielded a normal cell-cycle profile as it produces DNA double-strand breaks (DSBs) at all cell-cycle stages (Supplementary Figure 1A). Importantly, both treatments generated DNA damage effectively, as evidenced by robust γH2AX production and strong phosphorylation of p53 Ser-15 and SMC1 Ser-966 (Figure 1A). Next, we subjected samples from mock and DNA-damage-treated cells to western immunoblotting with a panel of 32 commercially available antibodies against known histone modifications (Figure 1C; Supplementary Table 1). To only analyse chromatin-associated histones and to lower non-specific antibody staining, we used acid-extracted histones (Shechter *et al*, 2007). Furthermore, although commercially available antibodies against histone PTMs are generally assumed to be highly specific, we included bacterially produced recombinant core histones that lack PTMs in our screen to assess whether any of the antibodies cross-reacted with unmodified histones (Supplementary Figure 1B). Thus, each antibody was tested for reactivity against four samples: one comprised of recombinant histones H2A, H2B, H3.1 and H4; one derived from mock-treated cells; one derived from HU-treated cells and one derived from phleomycin-treated cells. Importantly, samples contained very similar amounts of histone proteins as determined by Coomassie staining (Figure 1B).

As shown in Figure 1C, results from the screen fell into four distinct categories. Category I consisted of three antibodies that recognized recombinant histones and three antibodies that recognized PTMs on a different histone than the antibody was raised against, and were, therefore, deemed non-specific. Category II consisted of 10 antibodies whose signals were unaffected by DNA damage. Category III contained eight antibodies whose signals changed in response to DNA damage, but differed in their responses to HU and phleomycin. Category IV comprised antibodies whose signals changed similarly in response to both HU and phleomycin treatment. This latter group consisted of antibodies directed against dimethylated histone H3 Arg-2 (H3R2Me2), acetylated H3 Lys-9 (H3K9Ac), acetylated H3 Lys-14 (H3K14Ac), acetylated H3 Lys-56 (H3K56Ac), phosphorylated H3 Ser-10 (H3S10p), phosphorylated H3 Ser-28 (H3S28p) and phosphorylated H3.3 Ser-31 (H3S31p). We selected this group for further investigation as these histone marks were similarly responsive to both replicative and DSB-induced DNA damage. In addition, although the signal for H3 phosphorylation on Thr-11 (H3T11p) did not change appreciably in the initial screen, we included this modification in our subsequent studies as it has recently been linked with the DDR (Shimada *et al*, 2008).

Analysis of histone PTMs after DNA damage and throughout the cell cycle

To substantiate and expand on the above findings, histone PTMs selected for further investigation were analysed for their responses to various DNA-damaging agents including phleomycin, IR, UV, methylmethane sulfonate (MMS), camptothecin (CPT) and hydrogen peroxide (H_2O_2). In these experiments, no reproducible changes in H3K14Ac and H3R2Me2 levels were observed after DNA-damage induction in U2OS cells (Figure 2A, left panel; note that all treatments generated DNA damage, as evidenced by γH2AX production). As these PTMs also did not change appreciably on phleomycin treatment of human HeLa cells (Figure 2B, right panel), H3K14Ac and H3R2Me2 were not analysed further. In contrast to the above data, with the exception of H3T11p, all of the other histone PTMs selected for further investigation displayed varying decreases on DNA-damage induction both in U2OS and HeLa cells (Figure 2A). Notably, these data indicated that the profiles of H3 phosphorylation changes after DNA-damage induction were similar to one another and differed from the less pronounced reductions observed for H3K9Ac and H3K56Ac. For example, though CPT and IR had minor effects on H3K9Ac and K56Ac levels, these treatments substantially reduced the levels of H3 phosphorylations (Figure 2A). Collectively, these results suggested that changes in H3 phosphorylations and H3 acetylations define two distinct responses to DNA damage.

A major response to DNA damage is cell-cycle arrest (Harper and Elledge, 2007), raising the possibility that the histone PTM changes described above could reflect alterations in cell-cycle distribution rather than a response to DNA damage *per se*. To explore this possibility, we synchronized U2OS cells in G1/S with a double-thymidine block, released them back into the cell cycle and monitored cell-cycle progression by FACS analysis (Figure 2B, top panel). Western blotting analyses revealed that H3S10p, H3S28p and H3.3S31p were significantly increased in samples enriched for mitotic cells (Figure 2B, bottom panels, 12 and 14 h time points). Furthermore, and consistent with an earlier report (Shimada *et al*, 2008), H3T11p was detectable throughout the cell cycle, but increased during mitosis. In contrast, the variation of H3K9Ac and H3K56Ac throughout the cell cycle was minimal. This, therefore, suggested that the observed DNA-damage-dependent reductions of H3 phosphorylations might be a consequence of the levels of these PTMs being highest in mitosis, a cell-cycle stage that is lost after DNA damage (Hartwell and Weinert, 1989; Lukas *et al*, 2004). In contrast, these results indicated that the reduction of H3 acetylations in response to DNA damage could not simply be explained by DNA damage leading to altered cell-cycle distributions.

Analysis of histone H3 phosphorylations after DNA damage

As H3S10p, H3S28p and H3.3S31p occur primarily in mitosis (Figure 2B), this confounded our interpretation of their

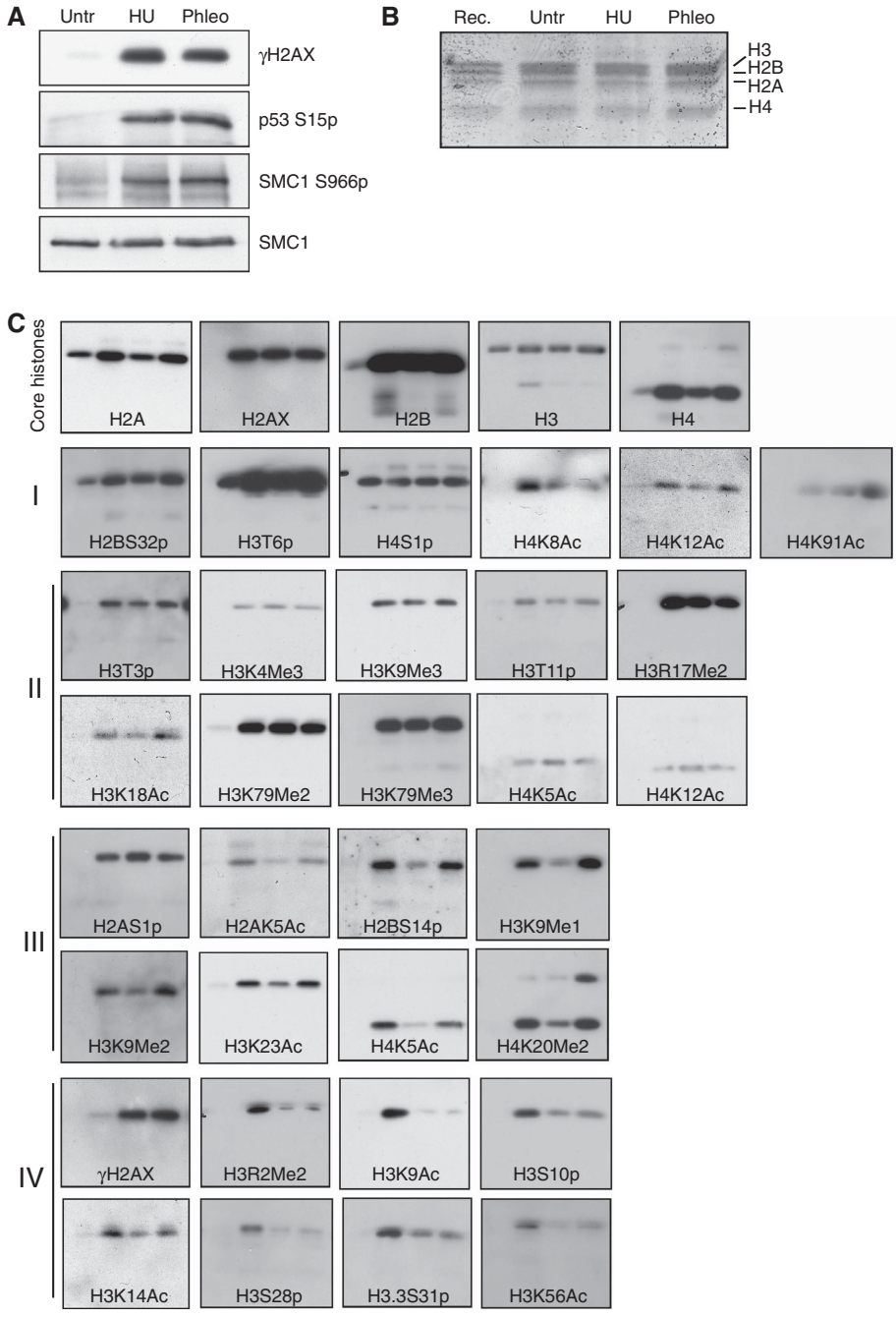

Figure 1 Screen for DNA-damage-responsive histone modifications. (**A**) U2OS cells were untreated (Untr) or treated with 2 mM HU for 24 h or with 60 μg/ml phleomycin (Phleo) for 2 h. Cells were split into two samples, one being used for the acid extraction of histones that were analysed in (B) and one sample for whole cell Laemmli extracts, which were analysed by western blotting with the indicated antibodies in (A). (**B**) Coomassie staining of recombinant histones (Rec) and acid-extracted histones from either untreated (Untr), HU-treated or phleo-treated U2OS cells. (**C**) Antibody-based screen for DNA-damage-responsive histone PTMs. Samples from (B) were used for western blot analysis with the antibodies described in Supplementary Table 1. The results were categorized as described in the text.

responses to DNA damage in asynchronous cell populations. To circumvent this limitation, we arrested cells in pro-metaphase with the microtubule poison nocodazole and ascertained the effect of DNA damage on H3 phosphorylations in a position of the cell cycle when these histone PTMs are highly abundant. For comparison, mitotically arrested cells were released into the cell cycle and then analysed for DNA-damage-induced changes in H3 phosphorylations when in the G1- and S-phases of the cell cycle (Figure 3A; Supplementary Figure 2). Significantly, none of the H3 phosphorylations analysed changed after DNA damage in nocodazole-arrested cells, even though the cells exhibited γH2AX induction (Figure 3A). Furthermore, cells in G1- and S-phase had substantially lower levels of H3 phosphorylations compared with nocodazole-arrested cells, supporting our findings that these histone marks are primarily mitotic. However, the almost undetectable levels of H3 phosphorylations in G1- and S-phase cells prevented us from concluding about their

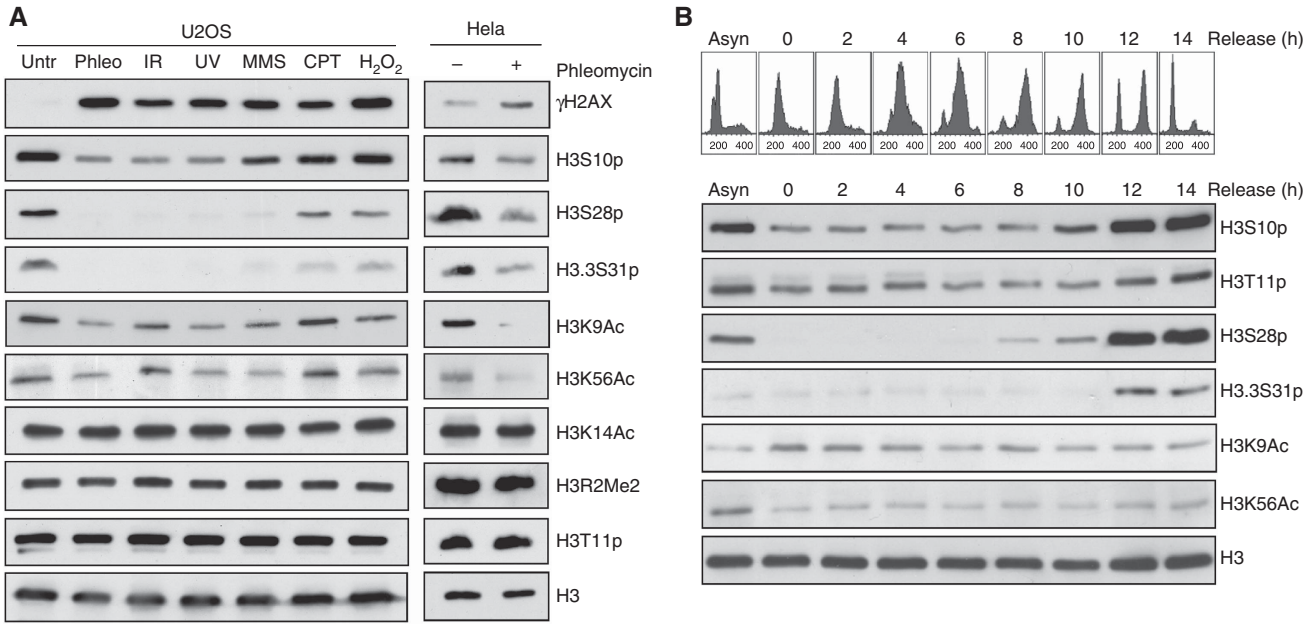

Figure 2 Analysis of DDR-responsive histone PTMs. (**A**) Analysis of histone PTMs in U2OS or Hela cells. Left panels, U2OS cells were treated with the indicated DNA-damaging agents (see Materials and methods for details) and analysed by western blotting of whole cell Laemmli extracts with the indicated antibodies. Right panels, Hela cells were untreated or treated with 60 μg/ml of phleomycin and analysed as described for U2OS cells. (**B**) Cell-cycle analysis of histone PTMs. U2OS cells were synchronized at the G1/S-transition by a double-thymidine procedure and subsequently released into the cell cycle. Samples were taken at indicated time points and cell-cycle distributions were determined by FACS analyses. A sample from asynchronous (Asyn) cells is shown as a control. These samples were additionally subjected to western blot analyses of whole cell Laemmli extracts and probed with the indicated antibodies.

behaviour after DNA damage in these stages of the cell cycle. Importantly, however, H3K9Ac and H3K56Ac were reduced after DNA damage in mitotic and G1/S-phase cells. Thus, H3K9 and H3K56 acetylation levels do not change dramatically throughout the cell cycle and, moreover, these modifications respond to DNA damage in various cell-cycle stages.

As a complementary approach to study H3 phosphorylations, we used immunofluorescence microscopy to visualize the effects of DNA damage on these PTMs in nocodazole-arrested cells (unfortunately, antibodies against H3K9Ac and H3K56Ac were not effective in immunofluorescence microscopy experiments, precluding their use in such analyses). Mitotic cells contain highly condensed chromosomes that stain brightly with DAPI compared with the larger, less brightly DAPI-stained, interphase cells. Consistent with our other data, H3S10p, H3T11p, H3S28p and H3.3S31p were highly enriched in mitotic cells compared with interphase cells (Figure 3B). However, neither the levels nor localization patterns of these modifications changed after DNA damage (Figure 3B), confirming that H3S10p, H3T11p, H3S28p and H3.3S31p are largely restricted to mitosis and are not perceptibly influenced by DNA damage in this phase of the cell cycle. By using higher exposures, we found that H3S10p and H3T11p were also detectable in interphase cells, where they co-localized in a punctate, nuclear-staining pattern. However, in line with our other data, this staining pattern was unchanged by DNA damage (Figure 3C). As a final approach to investigate whether H3T11p changes in response to DNA damage, we generated tracks containing high levels of local DNA damage in U2OS cell nuclei by laser microirradiation. This revealed that H3T11p was not recruited to nor excluded from the damaged regions, which were detected by staining for the DDR protein 53BP1 (Figure 3D; note the equivalent overall H3T11p-staining patterns in undamaged and micro-irradiated cells). Taken together, these findings led us to conclude that, like the other H3 phosphorylations studied, H3T11p is not an early DNA-damage-responsive histone modification in our system, which is in contrast to the conclusions presented in a recent report (Shimada *et al*, 2008).

H3K9Ac and H3K56Ac are DNA-damage-responsive histone PTMs

Histone modifications are best characterized for their involvement in transcription, and DNA damage can inhibit this process (Gentile *et al*, 2003; Kruhlak *et al*, 2007). We, therefore, concluded that the reductions we observed for H3K9Ac and H3K56Ac in response to DNA damage might reflect an indirect effect of transcriptional inhibition. To explore this possibility, we treated cells with the RNA polymerase II (Pol II) inhibitor 5,6-dichloro-1-beta-D-ribofuranosylbenzimidazole (DRB). This agent inhibits kinases responsible for phosphorylating Ser-2 and Ser-5 in the C-terminal domain of the Pol II largest subunit, thus preventing transcriptional elongation (Hirose and Ohkuma, 2007). As expected, DRB treatment reduced Pol II Ser-2 and Ser-5 phosphorylation and abolished the slower migrating, hyper-phosphorylated form of Pol II on SDS-polyacrylamide gels (Figure 4A; Supplementary Figure 3A). Effective transcriptional inhibition by DRB was also confirmed by the loss of fluorodeoxyuridine (FdU) incorporation (Supplementary Figure 3B). Significantly, we observed no decrease in H3K9Ac or H3K56Ac under these conditions (Figure 4A), indicating that

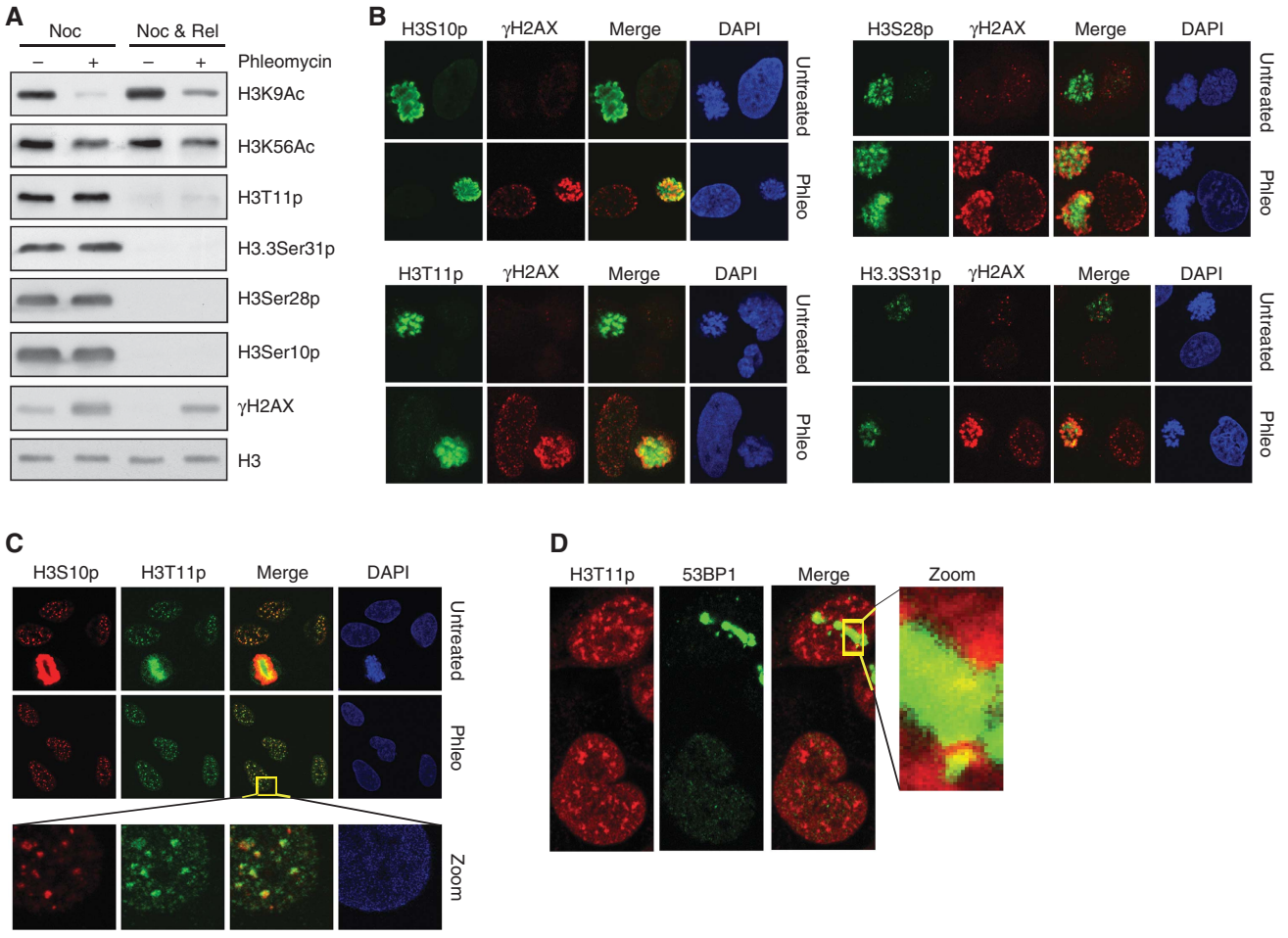

Figure 3 Mitotic H3 phosphorylations are unaltered by DNA damage. (**A**) H3 phosphorylation levels, but not acetylation levels, are unaffected by DNA damage. U2OS cells were arrested in pro-metaphase with nocodazole, then were either kept in nocodazole (Noc; M-phase) or released from nocodazole for 6 h (Noc & Rel; G1/S-phase) and subsequently either mock or phleomycin treated. Samples were analysed as in Figure 2. (**B**) Immunofluorescence analysis of H3 phosphorylations in mitosis. Nocodazole-arrested U2OS cells were left untreated or treated with phleomycin and analysed by immunofluorescence with the indicated antibodies. Induction of DNA damage was visualized by γH2AX staining and the nucleus by DAPI staining of DNA. (**C**) Analysis of H3S10p and H3T11p in interphase cells. U2OS cells were untreated or treated for 2 h with phleomycin and analysed by immunofluorescence for H3S10p and H3T11p. The enlarged section depicts punctuate co-localized staining of H3S10p and H3T11p. Note the loss of brightly stained mitotic cells in phleomycin-treated cell populations. (**D**) H3T11p is unaffected in cells containing concentrated tracks of DNA damage. U2OS cells were microirradiated to induce tracks containing DNA damage. Cells were allowed to recover for 2 h before fixation and subsequent dual staining for 53BP1 and H3T11p. Inset shows a zoomed section of the damaged area.

transcriptional inhibition alone does not appreciably impact on overall H3K9 and H3K56 acetylation levels.

If lowered H3K9Ac and K56Ac levels reflect the presence of DNA damage, one might expect that these histone PTMs would revert to normal levels once the DNA damage has been repaired. To test this, we treated cells acutely with phleomycin for 2 h and then collected the samples derived from whole cell Laemmli extracts at various time points after transferring the cells into fresh medium lacking phleomycin to allow DNA repair to occur. This revealed that H3K9Ac and H3K56Ac remained reduced compared with untreated samples for 2–4 h after DNA-damage induction, whereas γH2AX levels remained high during this time frame (Figure 4B; note that samples were equally loaded as revealed by immunoblotting for histone H3 and H3K14Ac, a non-DNA-damage-responsive histone modification). However, at 8 and 24 h after phleomycin treatment, γH2AX levels decreased, whereas H3K9 and H3K56 acetylation increased to levels nearing those in untreated cells (Figure 4B). Collectively, these results established that loss of γH2AX, which is associated with DNA repair in mammalian cells, correlates with the restoration of normal H3K9 and H3K56 acetylation levels.

We next determined the behaviour of H3K9Ac and H3K56Ac during a time course of chronic phleomycin treatment. Strikingly, this revealed that H3K9 and H3K56 acetylation could be reduced very rapidly, with near-maximal reductions being observed just 15 min after phleomycin addition (Figure 4C). We have been able to observe global reductions in acetylation levels of H3K9 and H3K56 more rapidly. Quantification of H3K9Ac and H3K56Ac showed an ~50% reduction in levels compared with untreated amounts (Supplementary Figure 4A). The amount of reduction in H3K9Ac and H3K56Ac after DNA damage at short-time intervals were consistent with the levels observed after 2 h of both phelomycin and UV treatments (compare Supplementary Figure 4A with 4B). In Figure 4C, we found that acetylation levels of H3K9 and H3K56 contrasted to γH2AX levels, which increased progressively over time to

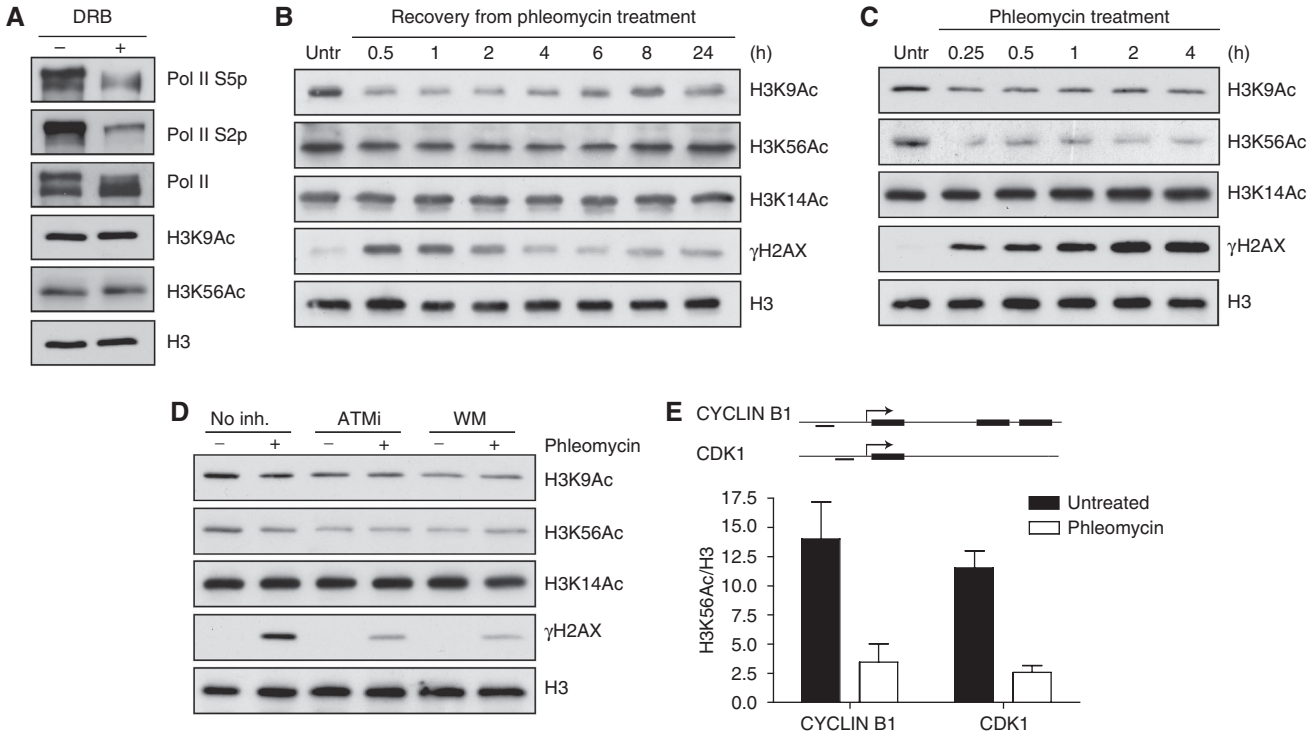

Figure 4 H3K9Ac and H3K56Ac decrease rapidly and reversibly upon DNA damage. (**A**) Transcriptional inhibition does not affect H3K9Ac and H3K56Ac levels. Cells were treated for 2 h with DRB, a Pol II transcription inhibitor, and analysed for H3K9Ac and H3K56Ac as described for Figure 2. (**B**) Dynamics of changes in H3K9Ac and H3K56Ac levels are reciprocal to those of γH2AX. Recovery dynamics of H3K9Ac and H3K56Ac levels were measured by acute treatment of U2OS cells with phleomycin for 2 h and subsequently releasing them into phleomycin-free medium. Samples were taken at the indicated time points and analysed using whole cell Laemmli extracts with the indicated antibodies. H3K14Ac was included to control for a DDR-independent histone acetylation, γH2AX to detect DNA-damage induction and H3 for loading. (**C**) H3K9Ac and H3K56Ac levels decrease rapidly upon DNA damage. U2OS cells were chronically treated with phleomycin and samples were taken at the indicated times and analysed as in A. (**D**) PIKK inhibition reduces H3K9 and H3K56 acetylation. U2OS cells were pre-incubated for 1 h with or without KU-55933, or wortmannin, then analysed as in A. (**E**) H3K56Ac levels are reduced at promoters of cell-cycle regulatory genes upon DNA damage. Schematic representation of CYCLIN B1 and *CDK1* genes showing positions analysed by ChIP followed by real-time qPCR. U2OS cells were untreated or treated with phleomycin or 2 h, before analyses by ChIP. Data represents percentage of IPed H3K56Ac signal normalized to IPed H3 signal at the indicated genomic loci. Data represent the average of three independent experiments and error bars show the standard deviation between these experiments.

reach maximum levels after around 2 h (this time-dependent increase was most likely due to the spreading of γH2AX surrounding DSBs, as well as constant DSB formation caused by the presence of phleomycin). Therefore, the reduction of H3K9Ac and H3K56Ac is quick and corresponds with the appearance of γH2AX, but is not directly proportional to γH2AX levels, as maximal reductions in H3K9Ac and H3K56Ac were reached before maximal levels of γH2AX were observed. Although other possibilities exist, these data suggest that the loss of H3K9Ac and H3K56Ac after DNA damage is not limited to sites of DNA damage, but rather occurs as a more global response to DNA damage.

Initiation of the DDR involves activation of the PIKK-family protein kinases, ATM, ATR and DNA-PK. As these kinases impinge on many processes, including transcription and checkpoint activation, and are required for effective DNA repair, they represented good candidates for initiating and transducing signals that would result in reduction of H3K9Ac and H3K56Ac levels. To investigate this possibility, we treated cells with the specific ATM inhibitor Ku-55933 (Hickson *et al*, 2004) or with the broad PIKK inhibitor wortmannin (Powis *et al*, 1994). Intriguingly, both inhibitors reproducibly reduced H3K9Ac and H3K56Ac levels in non-DNA-damage-treated cells (Figure 4D). Moreover, in the presence of these PIKK inhibitors, H3K9Ac and H3K56Ac levels were no longer reduced by phleomycin treatment (Figure 4D; as expected, γH2AX was generated on phleomycin treatment in a manner that was impaired by PIKK inhibition). Additionally, depletion of ATM using small-interfering RNAs (siRNAs) gave similar results (Supplementary Figure 5). One interpretation of these data is that ATM and possibly other PIKK-family members control H3K9Ac and H3K56Ac levels even in the absence of exogenous DNA damage. Alternatively, it may be that DNA damage affects these PTMs by PIKK-independent mechanisms and that treating cells with PIKK inhibitors leads to endogenous genotoxic stress that is, in itself, sufficient to trigger reduced H3K9Ac and H3K56Ac levels.

To use a more quantitative and complementary method for evaluating the effect of DNA damage on H3K56 acetylation, we sought to find regions in the genome that contained H3K56Ac and could, therefore, be analysed by chromatin immunoprecipitation (ChIP). It has been shown earlier that the *CDK1* and CYCLIN B1 promoter regions contain high levels of H3K9Ac, which are reduced after DNA damage (Shimada *et al*, 2008). As our data had established a strong correlation between H3K9Ac and H3K56Ac levels, we used ChIP to analyse the presence of H3K56Ac at the *CDK1* and

CYCLIN B1 promoter regions. As reported for H3K9Ac (Shimada *et al*, 2008), H3K56Ac was enriched on *CDK1* and CYCLIN B1 promoter regions as compared with the body of these genes (Figure 4E; Supplementary Figure 6A). Moreover, consistent with our western blotting data, we observed a 3–4 fold reduction in H3K56Ac levels on phleomycin-induced DNA damage using ChIP analysis (Figure 4E). Importantly, these results were not limited to DNA-damage-repressible genes as further analysis of additional, non-DNA-damage-responsive genes gave similar reductions in H3K56Ac levels upon DNA damage (Supplementary Figure 6B). To look at chromatin-bound histones using another method, we analysed Triton-resistant cell extracts either untreated or treated with phleomycin. Consistent with the other methods, this revealed that both H3K9Ac and H3K56Ac levels were reduced upon DNA damage (Supplementary Figure 7). Taken together, these findings, therefore, strongly support our other data indicating that levels of chromatin-associated H3K56Ac decrease when DNA is damaged.

Human GCN5/KAT2A acetylates H3K9 and H3K56

In yeast, acetylation of H3K56 is accomplished by Rtt109 (also termed KAT11), a HAT with no known homologues in higher eukaryotes (Collins *et al*, 2007; Driscoll *et al*, 2007; Han *et al*, 2007; Xhemalce *et al*, 2007). Although it has been generally assumed that H3K56Ac does not exist in human cells (Xu *et al*, 2005), the recent identification of human H3K56Ac by mass spectrometry and ChIP analysis has cast doubt on this assumption (Garcia *et al*, 2007; Xie *et al*, 2009). Interestingly, *Saccharomyces cerevisiae* Rtt109 was recently shown to additionally catalyse H3K9 acetylation, a histone PTM that is also generated by the HAT GCN5 (Fillingham *et al*, 2008). In light of this, and because we noted that both H3K9Ac and H3K56Ac lie within a Lys-Ser-Thr motif (Figure 5A), we speculated that human GCN5 (hGCN5, also named KAT2A) might acetylate H3K56. To test this idea, we purified recombinant hGCN5 and analysed its activity towards recombinant human histone H3.1 (Rec. H3), detecting products with antibodies directed against H3K9Ac or H3K56Ac. As positive controls, we also

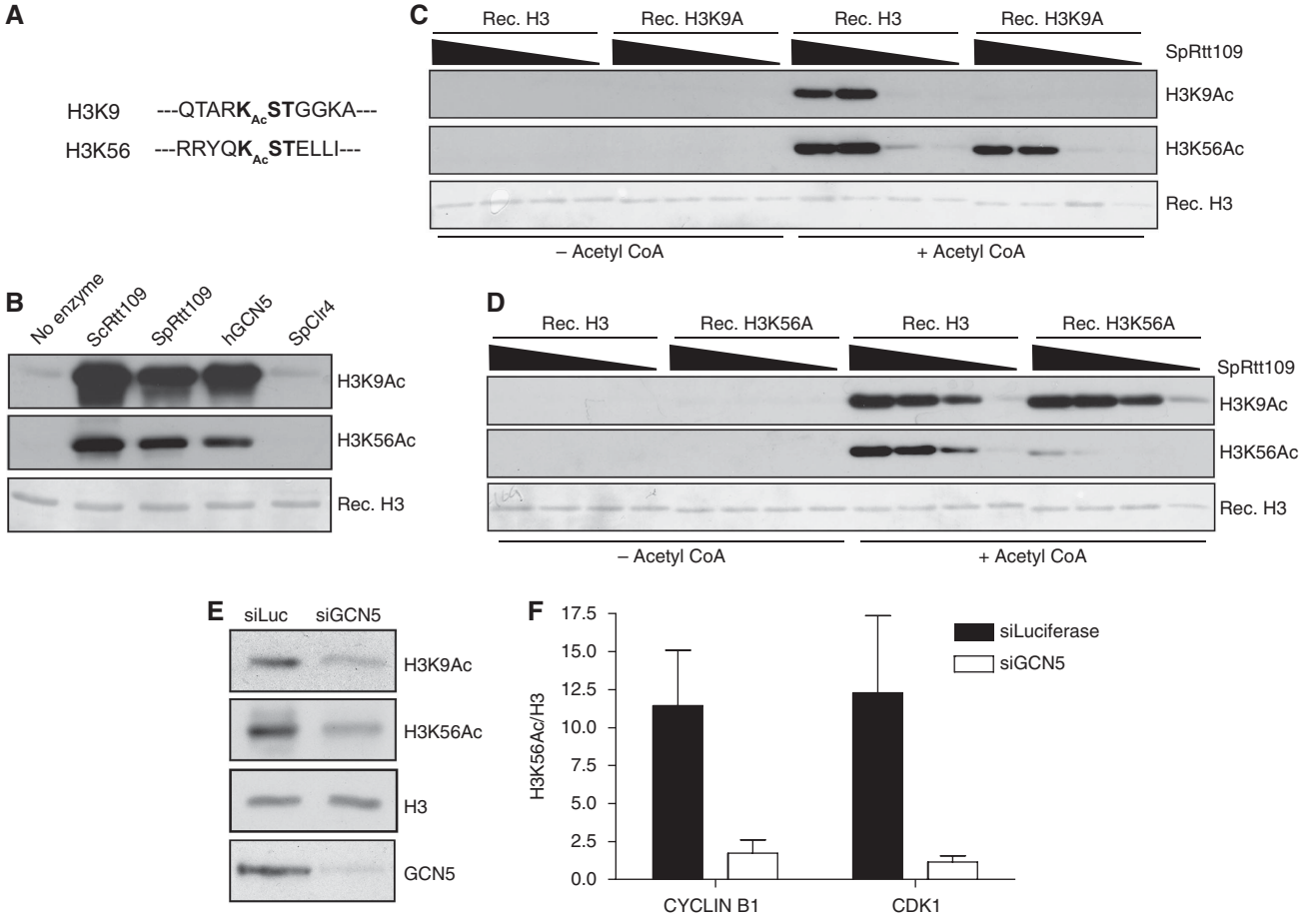

Figure 5 hGCN5 acetylates H3K9 and H3K56 *in vitro* and *in vivo*. (**A**) The H3K9 and H3K56 motifs share sequence similarity. (**B**) Human GCN5 acetylates H3K9 and H3K56 *in vitro*. HAT activity towards H3K9 and H3K56 was assessed with purified *S. cerevisiae* and *S. pombe* Rtt109 (ScRTT109 and SpRTT109, respectively) or human GCN5 (hGCN5) in an *in vitro* HAT-assay containing purified human recombinant histone H3.1 (Rec. H3) with subsequent analysis by western blotting with the indicated antibodies. SpClr4 was used as a non-HAT enzyme and a ponceau staining of Rec. H3 is shown as a loading control. (**C**) H3K9Ac antibody is specific. Purified SpRtt109 was incubated with Rec.H3 or Rec. H3 containing a Lys9 to Ala mutation (H3K9A) and analysed as in A. (**D**) H3K56Ac antibody is specific. Experiments were done as in B except Rec. H3K56A was used instead of Rec. H3K9A. (**E**) hGCN5 is involved in acetylation of H3K9 and H3K56 *in vivo*. U2OS cells were transfected with siRNAs against luciferase (siLuc) or GCN5 (siGCN5) and samples were analysed after 48 h by western blotting of whole cell Laemmli extracts with the indicated antibodies. (**F**) GCN5 depletion leads to the loss of H3K56Ac at promoters of cell-cycle regulatory genes. U2OS cells were transfected as in E and analysed as in Figure 4E.

carried out HAT assays with both *S. cerevisiae* and *Schizosaccharomyces pombe* Rtt109, and as a negative control, we used *S. pombe* histone methyl-transferase Clr4. Notably, as was the case for the two Rtt109 enzymes, hGCN5 mediated the acetylation of both H3K9 and H3K56 (Figure 5B). Because of the potential for antibody non-specificity, as well as cross-reactivity between H3K9Ac and H3K56Ac, we next carried out similar assays with wild-type histone H3 and with H3 derivatives bearing Lys-to-Ala mutations on either Lys-9 or Lys-56 (Rec. H3K9A and Rec. H3K56A, respectively). Importantly, these studies revealed that the H3K9Ac and H3K56Ac antibodies were indeed highly specific. Thus, the signal for H3K9Ac, but not H3K56Ac, was abolished when Rec. H3K9A was used as a substrate, whereas the signal for H3K56Ac, but not H3K9Ac, was lost when Rec. H3K56A was used (Figure 5C and D, respectively; note that no signal was observed when HAT assays were carried out in the absence of acetyl-CoA). Taken together, these data, therefore, established that hGCN5 can act as an H3K56 HAT *in vitro*.

To test whether hGCN5 contributes to H3K56 acetylation *in vivo*, we treated U2OS cells with a control siRNA or with a pool of siRNAs directed against hGCN5. Western blotting analysis revealed that hGCN5 depletion led to reproducible reductions in both H3K9Ac and H3K56Ac levels, indicating that hGCN5 promotes the formation of these PTMs *in vivo* (Figure 5E). As shown in Supplementary Figure 8A, similar effects were produced when we used a different siRNA targeting GCN5. Furthermore, hGCN5 depletion, using different siRNAs targeting GCN5, also led to a substantial reduction of H3K56Ac at the *CDK1* and CYCLIN B1 promoter regions as assessed by ChIP analysis (Figure 5F; Supplementary Figure 8B). Importantly, hGCN5 depletion did not result in DNA damage as assessed by γH2AX formation, suggesting that the observed decreases in H3K9Ac and H3K56Ac were specific and were not caused indirectly as a consequence of DNA-damage induction (Supplementary Figures 8C and 10). In addition, siGCN5 cells did not exhibit an aberrant cell-cycle profile or a loss in other transcriptionally active histone marks, suggesting that the reduced levels of H3K56Ac were a direct effect of GCN5 depletion and not an indirect effect caused by transcriptional repression (Supplementary Figures 9B and 10). As structural studies have suggested a homology between budding yeast Rtt109 and human p300, we analysed the effects of p300 depletion on the levels of H3K9Ac and H3K56Ac. Interestingly, knockdown of p300 resulted in a decrease in both H3K9Ac and H3K56Ac, although to a lesser extent than cells lacking GCN5 (Supplementary Figure 10). However, unlike GCN5, the depletion of p300 induced DNA damage as seen by an increase in γH2AX formation (Supplementary Figure 10). Unfortunately, this result prevents us from making a clear conclusion on the role of p300 in the acetylation of H3K56. However, taken together, our findings establish that hGCN5 is required for H3K56 acetylation *in vivo*. Although the incomplete nature of these reductions might reflect residual hGCN5 activity, it could also be that hGCN5 is just one of the several HATs that can target these sites, which is consistent with known redundancies between H3K9Ac HATs in various organisms (Kouzarides, 2007).

Discussion

Histone modifications have been proposed to dynamically regulate chromatin functions in all DNA-based processes (Kouzarides, 2007). We examined this hypothesis with respect to the DDR and report our findings from a large-scale antibody-based screen for histone modifications that are responsive to DNA damage. Perhaps surprisingly, the majority of histone modifications we analysed do not change detectably after genotoxic stress, even though these conditions are likely to affect transcription, a process intimately linked to the maintenance and utilization of histone PTMs (Berger, 2007; Kouzarides, 2007). Nonetheless, as discussed below, we were able to identify two classes of histone modifications whose global levels decrease upon DNA-damage induction: H3 phosphorylations on Ser-10, Ser-28 and Ser-31, together with H3 acetylations on Lys-9 and Lys-56.

Despite our initial findings and earlier reports implicating H3 phosphorylations in the DDR (Allison and Milner, 2003; Ito, 2007), our subsequent investigations have indicated that H3S10p, H3S28p and H3S31p are not primarily responsive to DNA damage *per se*, but, instead, their levels are reduced mainly by indirect mechanisms. Specifically, it seems that loss of these marks on DNA damage mainly reflects DNA damage inducing G2/M arrest, thus reducing the proportion of mitotic cells, a cell-cycle phase where these PTMs are most abundant. Consistent with this, we found that H3S10p, H3S28p and H3S31p levels did not change in response to DNA damage when we specifically analysed mitotic cell populations. Furthermore, and in contrast to an earlier study (Shimada *et al*, 2008), we do not detect a specific effect of DNA damage on H3T11p levels. Nevertheless, it is noteworthy that we have found that H3T11p co-localizes with H3S10p in interphase cells, raising the possibility that H3T11p is associated with transcription, a process linked with H3S10p in interphase (Cheung *et al*, 2000; Metzger *et al*, 2008; Shimada *et al*, 2008).

In contrast to the H3 phosphorylations, our data indicate that reductions in H3K9 and H3K56 acetylation in response to DNA damage do not simply reflect indirect, cell-cycle effects. Although the presence of H3K9Ac is well established in mammalian cells, characterization of H3K56Ac has thus far been limited to yeast, and its existence in human cells has been uncertain (Xu *et al*, 2005; Miller *et al*, 2006). Nevertheless, mass spectrometry-based studies have recently shown that H3K56 is both monomethylated and acetylated in human cells. Additionally, H3K56Ac has been found to mark both active and inactive genes in human embryonic stem cells (Xie *et al*, 2009). These facts, along with our data, clearly show the existence of H3K56Ac, which now raises questions about the functions of modified H3K56 in human cells (Peters *et al*, 2003; Freitas *et al*, 2004; Garcia *et al*, 2007). In yeast, H3K56Ac is abundant, occurs in S-phase on newly synthesized histones and is required for DNA-damage tolerance through a role in chromatin assembly (Masumoto *et al*, 2005; Driscoll *et al*, 2007; Xhemalce *et al*, 2007; Chen *et al*, 2008; Li *et al*, 2008). However, S-phase-specific histone acetylations have not been detected in human cells, suggesting that this function of H3K56Ac might have been lost in higher eukaryotes (Shahbazian and Grunstein, 2007). Additionally, our cell-cycle analysis suggests that H3K56Ac is not induced in S-phase in human cells, a finding shared

with another recent report on this mark in human cells (Xie *et al*, 2009). Notably, H3K56Ac has also been linked with transcription in yeast (Xu *et al*, 2005; Schneider *et al*, 2006), raising the possibility that such a function is conserved in human cells. Our data, along with a genome-wide analysis in human cells (Xie *et al*, 2009), has now established that H3K56Ac is enriched on promoter regions of both active and inactive genes (Figure 4E; Supplementary Figure 6). Global analysis of H3K9Ac places this histone PTM predominantly at promoter regions of active genes (Kouzarides, 2007; Wang *et al*, 2008), and it has been implicated in regulating transcriptional repression after DNA damage (Shimada *et al*, 2008). Therefore, given the similarity between the sequence contexts and physiological behaviours of H3K9Ac and H3K56Ac, and probably the HATs targeting these sites (see below), it is tempting to speculate that these marks share a common function. In support of this idea, we have found that, like H3K9Ac, H3K56Ac becomes diminished at promoter regions of both cell-cycle responsive and active genes in response to DNA damage (Figure 4E; Supplementary Figure 6).

While this paper was under review, a seemingly contradictory paper was published reporting that H3K56Ac increases in human cells in response to DNA damage and localizes to sites of damaged DNA (Das *et al*, 2009). One potential explanation for these discrepancies was that our experiments were performed with an antibody from Upstate directed against H3K56Ac, whereas Das *et al* used a different antibody from Epitomics. Additionally, our doses of DNA-damaging agents were orders of magnitude lower than those used in Das *et al*. For example, our treatments for HU and UV were 2 mM and 20 J/m^2, respectively, whereas Das *et al* used 150 mM HU and 49 995 J/m^2. Although these differences might have explained the differential effects reported by Das *et al* and ourselves, we have performed similar and additional experiments with the Epitomics antibody, and in no case have we been able to detect any increase of H3K56Ac after DNA damage or H3K56Ac localization with sites of DNA damage (JVT and KMM, unpublished data). Unfortunately, we are, therefore, unable at this time to offer an explanation for the discrepancies between our data and those of Das *et al*.

A key question arising from our work is which HAT(s) target H3K56 *in vivo*? The structure of Rtt109, the HAT that targets both H3K56 and H3K9 in yeast, has recently been solved (Fillingham *et al*, 2008) and is most similar to human p300 (Tang *et al*, 2008). Although p300, like hGCN5, can target lysines in the N-terminal tail of H3, it has poor *in vitro* activity towards H3K56 (Tang *et al*, 2008). Our *in vivo* analysis of p300 and its role in H3K56Ac were inconclusive as, although reductions in H3K56Ac and H3K9Ac were observed, cells lacking p300 exhibited DNA damage, which could explain the reduced levels of these histone marks in these cells (Supplementary Figure 10). The catalytic residues of *S. cerevisiae* Rtt109 required for its HAT activity have been identified (Tang *et al*). Surprisingly, *S. cerevisiae* Rtt109 shares only 27% identity with *S. pombe* Rtt109, the only other HAT for H3K56 that has been described to date, and the catalytic residues in *S. cerevisiae* Rtt109 are poorly conserved in human p300 (Xhemalce *et al*, 2007; Tang *et al*, 2008). Collectively, these data suggest that the HATs responsible for acetylation of H3K9 and H3K56 could be numerous and divergent; and it remains to be established whether there is a *bona fide* Rtt109 homologue in mammals. Regardless, our work has revealed that hGCN5 can promote the acetylation of H3K56, as well as H3K9Ac, in human cells. Notably, like H3K9Ac, hGCN5 has been implicated in the transcriptional repression of the cell-cycle regulated genes *CDK1* and CYCLIN B1 after DNA damage (Shimada *et al*, 2008). Our ChIP analyses of H3K56Ac at the promoters of these genes are consistent with H3K56Ac also being involved in this process, as both DNA damage and depletion of hGCN5 resulted in significant reductions of H3K56Ac on these promoters (Figures 4E and 5F). However, we also observe a reduction in H3K56Ac on promoters of active genes that are not repressed upon DNA damage (Supplementary Figure 6C) as well as a reduction in cells depleted of GCN5, whereas these cells were still able to cycle and had normal levels of CDK1, CYCLIN B1 and transcriptionally active histone marks (Supplementary Figure 9). Taken together, our data suggest that low levels of H3K56Ac do not correlate directly with repressed transcription, which is in accord with H3K56Ac being found on promoters of numerous genes regardless of their transcriptional status in human embryonic stem cells (Xie *et al*, 2009).

Taking the above issues into consideration, it will be of interest to determine whether the reductions of H3K9 and H3K56 acetylation in response to DNA damage are caused by DNA damage leading to the inhibition of hGCN5 or other HATs for these sites. In line with such an idea, ChIP data have shown that hGCN5 is lost from some promoter regions upon DNA damage (Shimada *et al*, 2008). However, global or microirradiation-induced DNA damage did not have a discernable effect on hGCN5 as assessed by immunofluorescence, which could suggest that only a subset of hGCN5 is affected by DNA damage (Supplementary Figure 8C and D). Therefore, the precise relationship between hGCN5 and the DDR awaits future investigation. Alternatively, or in addition, DNA damage might enhance the activities of HDAC enzymes for H3K9Ac and H3K56Ac. In this regard, it is noteworthy that SIRT6, a member of the Sirtuin family of HDACs, deacetylates H3K9Ac in mammalian cells (Michishita *et al*, 2008) and that H3K56Ac is also deacetylated by Sirtuins in yeast (Celic *et al*, 2006; Maas *et al*, 2006). However, cells lacking SIRT6 displayed normal global H3K9Ac levels (Michishita *et al*, 2008), and in addition, we found that over-expression or siRNA-mediated depletion of SIRT6 had no detectable effect on H3K9Ac or H3K56Ac levels in our system (JVT and KMM, unpublished data). Additionally, though the use of different classes of HDAC inhibitors all led to increased H3K9 and H3K56 acetylation levels, only minor increases were observed when using the Sirtuin-specific inhibitor Nicotinamide (Supplementary Figure 11). Collectively, these data allude to a redundancy of HDACs for H3K9Ac and H3K56Ac. Interestingly, in *S. pombe*, the HDAC Clr6 deacetylates H3K9, and mutation of Clr6 or its *S. cerevisiae* homologue Sin3, results in hyper-sensitivity to genotoxic stresses (Jazayeri *et al*, 2004; Nicolas *et al*, 2007). Thus, in systems where H3K9Ac and H3K56Ac have been studied, deregulation of these histone marks results in an inability to tolerate DNA damage. As subjecting human histone H3 to genetic analyses is difficult, defining the precise functions of H3K9Ac and H3K56Ac in the DDR is likely to represent a formidable challenge.

Another scenario that could account for the reduction of H3K9Ac and H3K56Ac in response to DNA damage is histone eviction coupled with degradation. In yeast, histone turnover has been shown to occur rapidly in promoter regions (Dion *et al*, 2007). As we have found that H3K9Ac and H3K56Ac are enriched in promoter regions (Figures 4E and 5F), these acetylations could influence this process. However, the dynamics of histone turnover, either in the absence or presence of DNA damage, in human cells, is unknown (Wang *et al*, 2008). Additionally, poly-ubiquitylation of H3 occurs after DNA damage in human cells and ubiquitylation of H3/H4 was shown to destabilize nucleosomes *in vitro*, which could favour eviction with subsequent degradation (Wang *et al*, 2006). Together, such events could potentially regulate H3K9Ac and H3K56Ac levels after DNA damage.

Our work raises the important question of why DNA damage specifically decreases the global levels of H3K9Ac and H3K56Ac? Global responses to DNA damage have been documented in various systems and have been shown to impact on phenomena such as chromatin relaxation, genome-wide sister-chromatid cohesion, transcriptional repression as well as acetylation/deacetylation of proteins (including histones) (Ramanathan and Smerdon, 1986; Gentile *et al*, 2003; Ziv *et al*, 2006; Strom *et al*, 2007; Unal *et al*, 2007). It will, therefore, be interesting to investigate the potential role of H3K9Ac and H3K56Ac in these processes both in the presence or absence of genotoxic stress. As HDAC inhibitors are promising cancer therapeutic agents that have been shown to radio-sensitize cancer cells (Cerna *et al*, 2006; Camphausen and Tofilon, 2007), understanding the interplay between DNA damage and histone acetylation could give important insights into the mechanisms of these emerging drugs for the treatment of cancers.

Materials and methods

Cell culture, reagents and treatments

Human U2OS and HeLa cells were grown in Dulbecco's modified Eagle's medium (DMEM) supplemented with 10% foetal bovine serum, 100 U/ml penicillin, 100 mg/ml streptomycin and 2 mM L-glutamine. Drug treatments were with MMS (Sigma, 3 mM, 60 min), phleomycin (Sigma, 60 μg/ml, 2 h), H_2O_2 (VWR International, 500 μM, 30 min) or CPT (Sigma, 1 μM, 60 min). Cells were exposed to 15 Gy of IR with a ^{137}Cs source and subsequently placed in a 37°C incubator for recovery for 1 h. UV treatments were at 20 J/m^2 followed by recovery for 1 h. Wortmannin (Alexis Biochemicals, 50 mM, 0.5 h pre-incubation) and ATM inhibitor (KU-55933, KuDOS Pharmaceuticals, Cambridge, UK, 25 mM, 0.5 h pre-incubation) were used to inhibit PIKKs. HDAC inhibitors were added for 24 h and final concentrations were as follows: sodium butyrate (5 mM), TSA (1.3 μM) or Nicotinamide (20 mM). Primary histone antibodies used in this study are listed in Supplementary Table 1. Cell-cycle analyses of U2OS cells were done with a double-thymidine block-and-release procedure. To arrest in G1/S, cells were treated for 18 h with 3 mM thymidine (Sigma). Cells were washed three times with PBS and placed in fresh medium to release cells back into the cell cycle. After 12 h, cells were again treated with 3 mM thymidine containing DMEM for an additional 18 h. Cells were again released into the cell cycle by washing three times with PBS and adding fresh medium, and samples were taken at the indicated time points by harvesting cells with trypsin. One-fifth of the cells was used for FACS analysis and the rest was subjected to Laemmli lysis buffer to generate whole cell extracts (WCEs) (see below). For prometaphase synchronization, cells were incubated for 18 h with DMEM medium containing 0.1 μg/ml of nocodazole (Fisher Scientific). Cells were harvested as described above and analysed by FACS and western blotting with the indicated antibodies. Transcriptional inhibition was accomplished by treating cells for 2 h with the RNA Pol II inhibitor DRB (75 mM stock in DMSO) at a final concentration of 100 μM. Cells were either analysed by western blotting with the indicated antibodies or analysed by immunofluorescence. For immunofluorescence, after 2 h of DRB treatment, cells were incubated in 1 mM 5 FdU (50 mM stock in PBS) for 15 min. Cells were washed three times in PBS followed by fixation in 2% paraformaldehyde (PBS) for 20 min at room temperature, then washed three times with PBS and then permeabilized with 0.2% Triton in PBS for 5 min at room temperature. Cells were washed again three times in PBS, blocked for 20 min in PBS containing 3% BSA and then incubated in anti-BrdU antibody for 1 h at room temperature. Cells were then analysed as described for immunofluorescence (see below). Non-histone primary antibodies used were p53 Ser15-p (Cell Signaling), SMC1 Ser966-p (Bethyl Laboratories), SMC1 (Bethyl Laboratories), 53BP1 (Novus Biologicals), GCN5 (Cell Signaling), BrdU (Sigma), RNA Pol II (Santa Cruz), Pol II Ser2-p (Abcam), Pol II Ser5-p (Abcam), CHK2 (Cell Signaling), CHK2 T68p (Cell Signaling), ATM (kindly provided by Yossi Shiloh's Lab), p300 (Insight Biotechnology), CYCLIN-B1 (Pharmagen) and CDK1 (CRUK).

WCEs, site-directed mutagenesis and histone purifications

For WCEs, cells were washed once with PBS and collected by trypsinization and centrifugation. Pellets were resuspended in Laemmli buffer (4% SDS, 20% glycerol and 120 mM Tris [pH 6.8]) and sheared through a 23-guage needle, boiled for 5 min at 95°C and again sheared with a needle. Triton-resistant extracts were made by washing cells once with PBS followed by 5 min on ice in CSK buffer (10 mM PIPES pH 6.8, 100 mM NaCl, 300 mM sucrose, 3 mM $MgCl_2$, 1 mM EGTA, 0.5% TritonX-100). Cells were washed three times in cold-PBS, scraped in Laemmli buffer, sheared through a 23-gauge needle and finally boiled for 5 min before loading. Human core histones, H2A, H2B, H3.1 and H4 were cloned into pET21 and purified from *Escherichia coli* inclusion bodies as described earlier (Luger *et al*, 1999). Lys9 and Lys56 were mutated in H3.1 by standard techniques and mutated proteins purified as for wild-type H3.1. Acid extraction of histones was essentially performed as described (Shechter *et al*, 2007). Briefly, approximately 5×10^6 cells were collected by trypsinization and centrifugation, washed once with PBS, then the cell pellet was resuspended in 1 ml of hypotonic lysis buffer (10 mM Tris pH 8.0, 1 mM KCl, 1.5 mM $MgCl_2$, 1 mM dithiothreitol, 10 mM Na-butyrate, 20 mM *N*-ethylmaleimide, phosphatase inhibitors and protease inhibitor cocktail) and incubated for 30 min at 4°C to promote hypotonic swelling. The cells were then recovered by centrifugation, resuspended in 400 μl of 0.4 M H_2SO_4 and incubated on a rotator for 30 min at 4°C. After centrifugation, the supernatant was dialysed overnight at 4°C against 4 l of distilled water supplemented with 40 μl of β-mercaptoethanol. Samples were analysed using standard western blotting techniques. Quantification was performed, if indicated, using a LI-COR Odyssey infrared imaging system (LI-COR Biosciences), where densitometry values were calculated for various histone marks and normalized to H3 values. Secondary antibody used for quantification was IRDye 680CW Donkey anti-rabbit (LI-COR Biosciences).

siRNA transfection

RNA-interference was performed with the HiPerfect (Qiagen) transfection reagent as suggested by the manufacturer. U2OS cells were transfected at 25% confluency with siGCN5 (CCUUAGAGGG AAUAAUAAA) or siGCN5 smartpool from Dharmacon, sip300 (AACCCCUCCUCUUCAGCACCA), siATM (GACUUUGGCUGUCAAC UUUCG) or siLuciferase (CGUACGCGGAAUACUUCGA) at a final concentration of 5 nM. Transfections were repeated after 24 h, and samples were taken after an additional 24 h for GCN5 and ATM siRNAs or 48 h for p300 siRNA. Western blot analyses with the indicated antibodies were performed to analyse depletion efficiency.

Chromatin immunoprecipitation

In vivo cross-linking, chromatin purification and immunoprecipitations were performed as described earlier (Orlando *et al*, 1997). The average fragment size of soluble chromatin fragments after sonication was ~500 bp. Antibodies used for immunoprecipitations are listed in Supplementary Table 1. Primers used for qPCR for different loci are listed in Supplementary Table 2.

Immunofluorescence microscopy

U2OS cells were grown on poly-L-lysine-treated coverslips. For induction of DNA damage, cells were incubated with 60 μg/ml phleomycin for 2 h. Pro-metaphase-arrested cells were obtained by overnight incubation in 0.1 μg/ml of nocodazole. Once treated, coverslips were washed once with 1 × PBS at room temperature. Cells were then pre-extracted by incubating the coverslips in CSK buffer (10 mM PIPES pH 6.8, 100 mM NaCl, 300 mM sucrose, 3 mM $MgCl_2$, 1 mM EGTA, 0.5% TritonX-100) for 5 min on ice. Cells were washed once in cold-PBS and fixed with 2% paraformaldehyde for 15 min at room temperature followed by three washes with 1 × PBS containing 0.1% Tween-20 (PBS-T) and subsequently blocked for 15 min at room temperature in blocking buffer (PBS-T, 3% BSA). Primary antibodies were incubated for 1 h at room temperature in the same buffer. Cells were washed three times in wash buffer (PBS-T) before incubation in the dark with Alexa-conjugated secondary antibodies (Molecular Probes) in blocking buffer for 1 h at room temperature. Cells were again washed three times in PBS-T followed by a final wash in PBS. The coverslips were then mounted on slides in Vectashield containing DAPI (Vector laboratories). Cells were imaged with an inverted FV1000 confocal microscope (Olympus). For GCN5 staining in Supplementary Figure 5, cells were not pre-extracted with CSK buffer, but were analysed identically as for DRB-treated cells (see above).

HAT activity assay

Experiments were performed essentially as described before (Driscoll *et al*, 2007). Recombinant *S. cerevisiae* RTT109, *S. pombe* Rtt109 and human GCN5 (ScRtt109, SpRtt109 and hGCN5, respectively) were purified as described before (Wang *et al*, 1997; Driscoll *et al*, 2007; Xhemalce *et al*, 2007). Purified *S. pombe* Clr4 (SpClr4) was kindly provided by B Xhemalce (T Kouzarides laboratory). Reactions contained 1 μg of recombinant human H3.1 and either 2 μg SpRtt109, 1.2 μg SpRtt109, 1.2 μg SpClr4, 0.4 μg hGCN5 or Rec. H3.1 alone. Reactions were incubated for 45 min at 30°C. Samples were boiled in an equal volume of 3 × loading buffer (150 mM Tris–HCl pH 6.8, 350 mM β-mercaptoethanol, 150 mM DTT, 6% SDS, 30% glycerol and 0.1% bromophenol blue) and one-tenth of each reaction was analysed by western blotting with the indicated antibodies.

Supplementary data

Supplementary data are available at *The EMBO Journal* Online (http://www.embojournal.org).

Acknowledgements

We thank the T Kouzarides laboratory, especially T Bartke, P Hurd and B Xhemalce, for providing reagents and technical support. We also thank P Hurd for input in the initial phase of the project, and C Green, P Huertas and B Xhemalce for critical reading of the manuscript. We thank all members of the Jackson laboratory for help and support, especially S Polo and A Kaidi for technical support. JT is supported by a UK Biotechnology and Biological Sciences Research Council (BBSRC) Cooperative Award in Science and Engineering (CASE) studentship with KuDOS Pharmaceuticals, and KM is supported by a European Community grant (DNA Repair) and a Wellcome Trust project grant (086861/Z/08/Z). Research in the SPJ laboratory is made possible by core infrastructure funding from Cancer Research UK, the Wellcome Trust and funding from the European Community (Integrated Project DNA Repair, LSHG-CT-2005-512113 and GENICA).

References

Aguilera A, Gomez-Gonzalez B (2008) Genome instability: a mechanistic view of its causes and consequences. *Nat Rev Genet* **9:** 204–217

Allison SJ, Milner J (2003) Loss of p53 has site-specific effects on histone H3 modification, including serine 10 phosphorylation important for maintenance of ploidy. *Cancer Res* **63:** 6674–6679

Bekker-Jensen S, Lukas C, Kitagawa R, Melander F, Kastan MB, Bartek J, Lukas J (2006) Spatial organization of the mammalian genome surveillance machinery in response to DNA strand breaks. *J Cell Biol* **173:** 195–206

Berger SL (2007) The complex language of chromatin regulation during transcription. *Nature* **447:** 407–412

Camphausen K, Tofilon PJ (2007) Inhibition of histone deacetylation: a strategy for tumor radiosensitization. *J Clin Oncol* **25:** 4051–4056

Celeste A, Fernandez-Capetillo O, Kruhlak MJ, Pilch DR, Staudt DW, Lee A, Bonner RF, Bonner WM, Nussenzweig A (2003) Histone H2AX phosphorylation is dispensable for the initial recognition of DNA breaks. *Nat Cell Biol* **5:** 675–679

Celic I, Masumoto H, Griffith WP, Meluh P, Cotter RJ, Boeke JD, Verreault A (2006) The sirtuins hst3 and Hst4p preserve genome integrity by controlling histone h3 lysine 56 deacetylation. *Curr Biol* **16:** 1280–1289

Cerna D, Camphausen K, Tofilon PJ (2006) Histone deacetylation as a target for radiosensitization. *Curr Top Dev Biol* **73:** 173–204

Chen CC, Carson JJ, Feser J, Tamburini B, Zabaronick S, Linger J, Tyler JK (2008) Acetylated lysine 56 on histone H3 drives chromatin assembly after repair and signals for the completion of repair. *Cell* **134:** 231–243

Cheung P, Tanner KG, Cheung WL, Sassone-Corsi P, Denu JM, Allis CD (2000) Synergistic coupling of histone H3 phosphorylation and acetylation in response to epidermal growth factor stimulation. *Mol Cell* **5:** 905–915

Collins SR, Miller KM, Maas NL, Roguev A, Fillingham J, Chu CS, Schuldiner M, Gebbia M, Recht J, Shales M, Ding H, Xu H, Han J, Ingvarsdottir K, Cheng B, Andrews B, Boone C, Berger SL, Hieter P, Zhang Z *et al.* (2007) Functional dissection of protein complexes involved in yeast chromosome biology using a genetic interaction map. *Nature* **446:** 806–810

Das C, Lucia MS, Hansen KC, Tyler JK (2009) CBP/p300-mediated acetylation of histone H3 on lysine 56. *Nature* (e-pub ahead of print 8 March 2009)

Dion MF, Kaplan T, Kim M, Buratowski S, Friedman N, Rando OJ (2007) Dynamics of replication-independent histone turnover in budding yeast. *Science* **315:** 1405–1408

Downs JA, Nussenzweig MC, Nussenzweig A (2007) Chromatin dynamics and the preservation of genetic information. *Nature* **447:** 951–958

Driscoll R, Hudson A, Jackson SP (2007) Yeast Rtt109 promotes genome stability by acetylating histone H3 on lysine 56. *Science* **315:** 649–652

Escargueil AE, Soares DG, Salvador M, Larsen AK, Henriques JA (2008) What histone code for DNA repair? *Mutat Res* **658:** 259–270

Fernandez-Capetillo O, Allis CD, Nussenzweig A (2004) Phosphorylation of histone H2B at DNA double-strand breaks. *J Exp Med* **199:** 1671–1677

Fillingham J, Recht J, Silva AC, Suter B, Emili A, Stagljar I, Krogan NJ, Allis CD, Keogh MC, Greenblatt JF (2008) Chaperone control of the activity and specificity of the histone H3 acetyltransferase Rtt109. *Mol Cell Biol* **28:** 4342–4353

Freitas MA, Sklenar AR, Parthun MR (2004) Application of mass spectrometry to the identification and quantification of histone post-translational modifications. *J Cell Biochem* **92:** 691–700

Garcia BA, Hake SB, Diaz RL, Kauer M, Morris SA, Recht J, Shabanowitz J, Mishra N, Strahl BD, Allis CD, Hunt DF (2007) Organismal differences in post-translational modifications in histones H3 and H4. *J Biol Chem* **282:** 7641–7655

Gentile M, Latonen L, Laiho M (2003) Cell cycle arrest and apoptosis provoked by UV radiation-induced DNA damage are transcriptionally highly divergent responses. *Nucleic Acids Res* **31:** 4779–4790

Groth A, Rocha W, Verreault A, Almouzni G (2007) Chromatin challenges during DNA replication and repair. *Cell* **128:** 721–733

Gupta A, Sharma GG, Young CS, Agarwal M, Smith ER, Paull TT, Lucchesi JC, Khanna KK, Ludwig T, Pandita TK (2005) Involvement of human MOF in ATM function. *Mol Cell Biol* **25:** 5292–5305

Han J, Zhou H, Horazdovsky B, Zhang K, Xu RM, Zhang Z (2007) Rtt109 acetylates histone H3 lysine 56 and functions in DNA replication. *Science* **315:** 653–655

Harper JW, Elledge SJ (2007) The DNA damage response: ten years after. *Mol Cell* **28:** 739–745

Hartwell LH, Weinert TA (1989) Checkpoints: controls that ensure the order of cell cycle events. *Science* **246:** 629–634

Hickson I, Zhao Y, Richardson CJ, Green SJ, Martin NM, Orr AI, Reaper PM, Jackson SP, Curtin NJ, Smith GC (2004) Identification and characterization of a novel and specific inhibitor of the ataxia-telangiectasia mutated kinase ATM. *Cancer Res* **64:** 9152–9159

Hirose Y, Ohkuma Y (2007) Phosphorylation of the C-terminal domain of RNA polymerase II plays central roles in the integrated events of eucaryotic gene expression. *J Biochem* **141:** 601–608

Huen MS, Grant R, Manke I, Minn K, Yu X, Yaffe MB, Chen J (2007) RNF8 transduces the DNA-damage signal via histone ubiquitylation and checkpoint protein assembly. *Cell* **131:** 901–914

Ito T (2007) Role of histone modification in chromatin dynamics. *J Biochem* **141:** 609–614

Jazayeri A, McAinsh AD, Jackson SP (2004) Saccharomyces cerevisiae Sin3p facilitates DNA double-strand break repair. *Proc Natl Acad Sci USA* **101:** 1644–1649

Kolas NK, Chapman JR, Nakada S, Ylanko J, Chahwan R, Sweeney FD, Panier S, Mendez M, Wildenhain J, Thomson TM, Pelletier L, Jackson SP, Durocher D (2007) Orchestration of the DNA-damage response by the RNF8 ubiquitin ligase. *Science* **318:** 1637–1640

Kouzarides T (2007) Chromatin modifications and their function. *Cell* **128:** 693–705

Kruhlak M, Crouch EE, Orlov M, Montano C, Gorski SA, Nussenzweig A, Misteli T, Phair RD, Casellas R (2007) The ATM repair pathway inhibits RNA polymerase I transcription in response to chromosome breaks. *Nature* **447:** 730–734

Li Q, Zhou H, Wurtele H, Davies B, Horazdovsky B, Verreault A, Zhang Z (2008) Acetylation of histone H3 lysine 56 regulates replication-coupled nucleosome assembly. *Cell* **134:** 244–255

Luger K, Rechsteiner TJ, Richmond TJ (1999) Expression and purification of recombinant histones and nucleosome reconstitution. *Methods Mol Biol* **119:** 1–16

Lukas J, Lukas C, Bartek J (2004) Mammalian cell cycle checkpoints: signalling pathways and their organization in space and time. *DNA Repair (Amst)* **3:** 997–1007

Maas NL, Miller KM, DeFazio LG, Toczyski DP (2006) Cell cycle and checkpoint regulation of histone H3 K56 acetylation by Hst3 and Hst4. *Mol Cell* **23:** 109–119

Mailand N, Bekker-Jensen S, Faustrup H, Melander F, Bartek J, Lukas C, Lukas J (2007) RNF8 ubiquitylates histones at DNA double-strand breaks and promotes assembly of repair proteins. *Cell* **131:** 887–900

Masumoto H, Hawke D, Kobayashi R, Verreault A (2005) A role for cell-cycle-regulated histone H3 lysine 56 acetylation in the DNA damage response. *Nature* **436:** 294–298

Matsuoka S, Ballif BA, Smogorzewska A, McDonald III ER, Hurov KE, Luo J, Bakalarski CE, Zhao Z, Solimini N, Lerenthal Y, Shiloh Y, Gygi SP, Elledge SJ (2007) ATM and ATR substrate analysis reveals extensive protein networks responsive to DNA damage. *Science* **316:** 1160–1166

Metzger E, Yin N, Wissmann M, Kunowska N, Fischer K, Friedrichs N, Patnaik D, Higgins JM, Potier N, Scheidtmann KH, Buettner R, Schule R (2008) Phosphorylation of histone H3 at threonine 11 establishes a novel chromatin mark for transcriptional regulation. *Nat Cell Biol* **10:** 53–60

Michishita E, McCord RA, Berber E, Kioi M, Padilla-Nash H, Damian M, Cheung P, Kusumoto R, Kawahara TL, Barrett JC, Chang HY, Bohr VA, Ried T, Gozani O, Chua KF (2008) SIRT6 is a histone H3 lysine 9 deacetylase that modulates telomeric chromatin. *Nature* **452:** 492–496

Miller KM, Maas NL, Toczyski DP (2006) Taking it off: regulation of H3 K56 acetylation by Hst3 and Hst4. *Cell Cycle* **5:** 2561–2565

Nicolas E, Yamada T, Cam HP, Fitzgerald PC, Kobayashi R, Grewal SI (2007) Distinct roles of HDAC complexes in promoter silencing, antisense suppression and DNA damage protection. *Nat Struct Mol Biol* **14:** 372–380

Orlando V, Strutt H, Paro R (1997) Analysis of chromatin structure by *in vivo* formaldehyde cross-linking. *Methods* **11:** 205–214

Peters AH, Kubicek S, Mechtler K, O'Sullivan RJ, Derijck AA, Perez-Burgos L, Kohlmaier A, Opravil S, Tachibana M, Shinkai Y, Martens JH, Jenuwein T (2003) Partitioning and plasticity of repressive histone methylation states in mammalian chromatin. *Mol Cell* **12:** 1577–1589

Powis G, Bonjouklian R, Berggren MM, Gallegos A, Abraham R, Ashendel C, Zalkow L, Matter WF, Dodge J, Grindey G *et al* (1994) Wortmannin, a potent and selective inhibitor of phosphatidylinositol-3-kinase. *Cancer Res* **54:** 2419–2423

Ramanathan B, Smerdon MJ (1986) Changes in nuclear protein acetylation in u.v.-damaged human cells. *Carcinogenesis* **7:** 1087–1094

Rogakou EP, Pilch DR, Orr AH, Ivanova VS, Bonner WM (1998) DNA double-stranded breaks induce histone H2AX phosphorylation on serine 139. *J Biol Chem* **273:** 5858–5868

Schneider J, Bajwa P, Johnson FC, Bhaumik SR, Shilatifard A (2006) Rtt109 is required for proper H3K56 acetylation: a chromatin mark associated with the elongating RNA polymerase II. *J Biol Chem* **281:** 37270–37274

Shahbazian MD, Grunstein M (2007) Functions of site-specific histone acetylation and deacetylation. *Annu Rev Biochem* **76:** 75–100

Shechter D, Dormann HL, Allis CD, Hake SB (2007) Extraction, purification and analysis of histones. *Nat Protoc* **2:** 1445–1457

Shimada M, Niida H, Zineldeen DH, Tagami H, Tanaka M, Saito H, Nakanishi M (2008) Chk1 is a histone H3 threonine 11 kinase that regulates DNA damage-induced transcriptional repression. *Cell* **132:** 221–232

Strom L, Karlsson C, Lindroos HB, Wedahl S, Katou Y, Shirahige K, Sjogren C (2007) Postreplicative formation of cohesion is required for repair and induced by a single DNA break. *Science* **317:** 242–245

Stucki M, Jackson SP (2006) gammaH2AX and MDC1: anchoring the DNA-damage-response machinery to broken chromosomes. *DNA Repair (Amst)* **5:** 534–543

Tang Y, Holbert MA, Wurtele H, Meeth K, Rocha W, Gharib M, Jiang E, Thibault P, Verrault A, Cole PA, Marmorstein R (2008) Fungal Rtt109 histone acetyltransferase is an unexpected structural homolog of metazoan p300/CBP. *Nat Struct Mol Biol* **15:** 998

Thiriet C, Hayes JJ (2005) Chromatin in need of a fix: phosphorylation of H2AX connects chromatin to DNA repair. *Mol Cell* **18:** 617–622

Unal E, Heidinger-Pauli JM, Koshland D (2007) DNA double-strand breaks trigger genome-wide sister-chromatid cohesion through Eco1 (Ctf7). *Science* **317:** 245–248

Wang H, Zhai L, Xu J, Joo HY, Jackson S, Erdjument-Bromage H, Tempst P, Xiong Y, Zhang Y (2006) Histone H3 and H4 ubiquitylation by the CUL4-DDB-ROC1 ubiquitin ligase facilitates cellular response to DNA damage. *Mol Cell* **22:** 383–394

Wang L, Mizzen C, Ying C, Candau R, Barlev N, Brownell J, Allis CD, Berger SL (1997) Histone acetyltransferase activity is conserved between yeast and human GCN5 and is required for complementation of growth and transcriptional activation. *Mol Cell Biol* **17:** 519–527

Wang Z, Zang C, Rosenfeld JA, Schones DE, Barski A, Cuddapah S, Cui K, Roh TY, Peng W, Zhang MQ, Zhao K (2008) Combinatorial patterns of histone acetylations and methylations in the human genome. *Nat Genet* **40:** 897–903

Xhemalce B, Miller KM, Driscoll R, Masumoto H, Jackson SP, Kouzarides T, Verreault A, Arcangioli B (2007) Regulation of histone H3 lysine 56 acetylation in Schizosaccharomyces pombe. *J Biol Chem* **282:** 15040–15047

Xie W, Song C, Young NL, Sperling AS, Xu F, Sridharan R, Conway AE, Garcia BA, Plath K, Clark AT, Grunstein M (2009) Histone h3 lysine 56 acetylation is linked to the core transcriptional network in human embryonic stem cells. *Mol Cell* **33:** 417–427

Xu F, Zhang K, Grunstein M (2005) Acetylation in histone H3 globular domain regulates gene expression in yeast. *Cell* **121:** 375–385

Ziv Y, Bielopolski D, Galanty Y, Lukas C, Taya Y, Schultz DC, Lukas J, Bekker-Jensen S, Bartek J, Shiloh Y (2006) Chromatin relaxation in response to DNA double-strand breaks is modulated by a novel ATM- and KAP-1 dependent pathway. *Nat Cell Biol* **8:** 870–876